




Long-term Speckle Interferometric Monitoring of Binary Systems: 2007–2023 Positional Measurements and Orbits of Seven Objects

Arina Mitrofanova , Vladimir Dyachenko, Anatoly Beskakotov, Yuri Balega, Alexander Maksimov, and Denis Rastegaev

Special Astrophysical Observatory, 369167 Nizhnij Arkhyz, Russia; mitrofanova@sao.ru

Received 2024 July 3; revised 2024 July 28; accepted 2024 August 6; published 2024 September 17

Abstract

The results of seventeen years of speckle interferometric monitoring of seven objects (Chara 122Aa, GJ 3010, HIP 1987, GJ 3076, HIP 11253, HIP 11352, and HIP 14929) are presented. Observational data were obtained at the 6 m Big Telescope Alt-azimuthal Special Astrophysical Observatory of the Russian Academy of Science (BTA SAO RAS) from 2007 to the present. Analysis of previously published and new measurements made it possible to construct completely new orbits for Chara 122Aa, HIP 11253, and HIP 14929. The orbit of GJ 3076 cannot be constructed accurately due to the large influence of the weights assigned to the measurements. The resulting orbital solutions are classified based on a grading scheme suggested by W.I. Hartkopf, B.D. Mason and C.E. Worley; most orbits are “definitive” (Grade 1). The mass sums and masses of components calculated by two independent methods using Hipparcos and Gaia DR2 and DR3 parallaxes were compared for the objects under study.

Key words: techniques: high angular resolution – (stars:) binaries: visual – stars: fundamental parameters – stars: low-mass – stars: solar-type

Materials only available in the [online version of record](#): machine-readable table

1. Introduction

One of the techniques for studying double and multiple systems is speckle interferometry. It was invented by Labeyrie (1970) and started to be applied in this area at 1–6 m telescopes (for example, Balega et al. 1984; Beddoes et al. 1976; Bonneau et al. 1980; McAlister 1977; Morgan et al. 1978; Tango et al. 1979; Tokovinin 1978; Weigelt 1978). The results of the Hipparcos mission (Perryman et al. 1997) made it possible to create samples of objects for speckle interferometric monitoring, which is currently ongoing (for example, Davidson et al. 2024; Horch et al. 2021; Hussein et al. 2024; Masda et al. 2023; Mason et al. 2023; Tokovinin et al. 2022; Vrijmoet et al. 2022). However, modern research is not only based on a large number of positional measurements, but the data from the Gaia mission are also of great importance (Gaia Collaboration et al. 2018, 2023).

The group of high resolution methods in astronomy at the Special Astrophysical Observatory of the Russian Academy of Sciences (SAO RAS) has a great foundation and more than thirty years of experience in conducting such research (starting with works by Balega & Balega 1985 and ending with ones by Mitrofanova et al. 2021, 2020a, 2020b). The study of seven systems (Chara 122Aa, GJ 3010, HIP 1987, GJ 3076, HIP 11253, HIP 11352, and HIP 14929) presented in the article is based on their speckle interferometric monitoring conducted by our team for 17 years (from 2007 to 2023). Section 2 provides a description of speckle interferometric observations and data

reduction results. Section 3 is dedicated to the construction, analysis, and classification of the orbital solutions obtained. A discussion is provided in Section 4.

2. Data reduction of Observations

Speckle interferometric observations were carried out in 2007–2023 at the Big Telescope Alt-azimuthal (BTA) of the SAO RAS utilizing a speckle interferometer (Maksimov et al. 2009). The standard detectors, exposure time, and number of images per series are used as in Mitrofanova et al. (2020b, 2020a, 2021). The following interference filters were used (central wavelength λ / bandpass $\Delta\lambda$): 550/20 nm, 550/50 nm, 600/40 nm, 700/50 nm, 800/100 nm and 900/80 nm. Most of the speckle images ($\sim 57\%$) were obtained under good weather conditions with seeing $1''$ – $2''$, $\sim 23\%$ of the observations were carried out under excellent weather conditions with seeing $<1''$, $\sim 10\%$ of the data were obtained under satisfactory weather conditions with seeing $2''$ – $2''.5$, and $\sim 10\%$ of the data—under bad weather conditions with seeing $>2''.5$.

The calibration methods for speckle interferometric images, which provide high measurement accuracy, are listed by Mitrofanova et al. (2020b). Positional parameters and magnitude differences were determined through the analysis of the power spectrum and the auto-correlation function of the speckle interferometric series described in Balega et al. (2002) and Pluzhnik (2005). The reconstruction of the position

Table 1
Positional Parameters and the Magnitude Differences

Object	Epoch (yr)	Telescope (diameter, m)	$\lambda/\Delta\lambda$ (nm)	θ°	σ_θ°	ρ (mas)	σ_ρ (mas)	Δm (mag)	$\sigma_{\Delta m}$ (mag)	References
Chara 122Aa	1986.8967	4	549/22	94.9		110				McAlister et al. (1989)
	1988.6552	4	549/22	90.5		108				McAlister et al. (1990)
	1988.8982	1.8	538/76	81.4		112				Fu et al. (1997)
	1989.7174	4	549/22	266.6		107				Hartkopf et al. (1992)
	1990.7548	4	549/22	261.4		103				Hartkopf et al. (1992)

Note. Table 1 is available in machine-readable form and lists the parameters published earlier by Balega et al. (2002, 2004, 2005, 2006b, 2007, 2013), Beuzit et al. (2004), Calissendorff et al. (2020, 2022), Cortés-Contreras et al. (2017), ESA (1997), Hartkopf et al. (1997, 2000), Horch et al. (1999, 2002, 2004, 2008, 2009, 2010, 2011, 2012, 2015, 2017, 2021), Janson et al. (2012, 2014a, 2014b), Kehrli et al. (2017), Mason et al. (2001), McAlister et al. (1993), Pluzhnik (2005), Riddle et al. (2015), Tokovinin et al. (2021).

(This table is available in machine-readable form in the [online article](#).)

of the secondary was carried out by the method of bispectral analysis (Lohmann et al. 1983).

Table 1 presents the observation log, as well as new and previously published positional parameters and the magnitude differences of the systems under study. The columns are object designation; epoch of observation in fractions of Besselian year; telescope diameter; bandpass or $\lambda/\Delta\lambda$; θ and σ_θ are the position angle of the secondary relative to the primary and its error respectively; ρ and σ_ρ are the separation between the two stars and its error respectively; Δm and $\sigma_{\Delta m}$ are the magnitude difference and its error respectively; and reference. The analysis of the magnitude differences from the data obtained in different epochs shows that the average population standard deviation of new measurements is about 0.09 mag.

3. Orbit Construction

The preliminary and final orbital solutions were constructed using the Monet method (Monet 1977) and the ORBIT software package (Tokovinin 1992), respectively. The quadrant ambiguities were found in the positions of previously published measurements. As a result, the values of their position angles were changed by $\pm 180^\circ$ (in Table 1, the values of the position angles correspond to the published data). These measurements are listed in an individual description below for each object under study.

Table 2 presents both our orbital parameters for the systems under study and those found in the literature. The columns give: (1) object designation; (2) the orbital period in years; (3) the epoch of periastron passage; (4) the eccentricity; (5) the semimajor axis in mas; (6) the longitude of the ascending node; (7) the argument of periastron; (8) the inclination; and (9) the reference for the calculation.

We use all the measurements obtained with different instruments and methods to construct the orbits. Since each measurement contributes to the orbital solution and has its systematic error, the corresponding weights were selected for them, depending on the values of the residuals and deviations

from the orbit (smaller weights are assigned to ones with large errors). Therefore, orbital residuals on ρ and θ can be higher than the estimates of uncertainties presented in Table 1.

To determine the fundamental parameters of systems and their components (masses, spectral types, and mass sum), we used two independent methods, which are described in detail by Mitrofanova et al. (2020b, 2020a, 2021). Hipparcos (van Leeuwen 2007) and Gaia DR2 and DR3 parallaxes (Gaia Collaboration et al. 2018, 2023) were used. To obtain the apparent magnitudes of HIP 1987 in the V band, we used photometric ratios and conversion rate from Busso et al. (2018). Table 3 lists the fundamental parameters of objects and their components. The columns give: (1) object designation; (2) the average magnitude difference of the components in the 550 bandpass (Δm_{550}); (3, 6) the absolute magnitudes of the components in V band (M_A and M_B); (4, 7) their spectral types (Sp_A and Sp_B); (5, 8) the masses of stars (\mathcal{M}_A and \mathcal{M}_B); (9) the mass sum of the components defined by orbital parameters by the first method ($\Sigma \mathcal{M}$); (10) parallax source (Hip is Hipparcos parallax, and DR2 and DR3 are parallaxes from the Gaia mission); and (11) reference. Below, we show the orbits obtained and discuss each system in detail.

Chara 122Aa (00^h04^m36^s.6 + 42°05′33″ 1; HD 225218) is a binary, discovered by McAlister et al. (1989), and its first orbital solution was constructed by Cvetković et al. (2008). During the orbit construction the quadrant ambiguities of the following published measurements were found: McAlister et al. (1989, 1990), Fu et al. (1997), McAlister et al. (1993), Hartkopf et al. (1997, 2000). The system was unresolved in 1994.8988 at 1 m Zeiss SAO RAS, as described by Balega et al. (1999), which is consistent with the periastron value obtained in this work. Due to changes in position angles from the literature, the orbit was improved significantly (Figure 1, top-left panel). To classify the orbits we used the factors described by Hartkopf et al. (2001), but for some of them visual inspection was sufficient. The residuals regarding the new orbital solution for Chara 122Aa are $\Delta\rho = 3.3$ mas and

Table 2
Orbital Parameters

Object	P_{orb} , year	T_0 , year	e	a , mas	Ω , °	ω , °	i , °	References
Chara 122Aa	70.12 ± 5.41	2050.07 ± 96	0.515 ± 0.027	165 ± 8	100.6 ± 0.6	295.1 ± 4.4	104.8 ± 0.6	Novakovic (2006) Cvetković et al. (2008)
	70.1		0.515	165	100.6		104.8	Tokovinin (2017)
	35.4 ± 0.6	2005.96 ± 0.06	0.818 ± 0.007	90 ± 2	133 ± 1	64 ± 1	119 ± 1	This work
GJ 3010	5.918 ± 0.017	2018.921 ± 0.173	0.106 ± 0.023	144.0 ± 4.6	83.61 ± 6.59	240.38 ± 17.17	145.67 ± 3.29	Vrijmoet et al. (2022)
	$5.92^{+0.01}_{-0.01}$	$2018.91^{+0.04}_{-0.01}$	$0.10^{+0.01}_{-0.01}$	$143.8^{+1.6}_{-0.8}$	$84.2^{+0.2}_{-1.6}$	-119^{+1}_{-4}	$145.3^{+0.7}_{-1.6}$	*Grid Calissendorff et al. (2022)
	$5.94^{+0.02}_{-0.01}$	$2018.95^{+0.09}_{-0.08}$	$0.08^{+0.01}_{-0.01}$	$144.4^{+2.5}_{-2.5}$	$88.0^{+6.7}_{-6.5}$	$-115.7^{+7.9}_{-8.4}$	$144.3^{+1.8}_{-1.7}$	*MCMC
	5.901 ± 0.005	2018.29 ± 0.04	0.086 ± 0.003	146.4 ± 0.6	85.4 ± 0.9	249 ± 2	140.1 ± 0.5	This work
HIP 1987	28.05 ± 0.46	1999.29 ± 0.55	0.481 ± 0.058	230 ± 8	96.1 ± 16.2	358.9 ± 15.7	164.0 ± 3.8	Cvetković (2011)
	27.8 ± 0.1	2026.94 ± 0.06	0.463 ± 0.007	224 ± 2	112 ± 8	14 ± 8	162 ± 2	This work
GJ 3076	41^{+20}_{-10}	$2031.75^{+0.12}_{-0.11}$	$0.3^{+0.3}_{-0.3}$	450^{+20}_{-10}	127^{+3}_{-3}	-84^{+25}_{-4}	62^{+10}_{-8}	*Grid Calissendorff et al. (2022)
	56^{+1}_{-15}	$2045.4^{+3.45}_{-2.3}$	$0.06^{+0.15}_{-0.04}$	437^{+15}_{-6}	$127.86^{+5.4}_{-5.4}$	-85^{+33}_{-14}	$51.05^{+6.41}_{-1.43}$	*MCMC
	54.2 ± 14.5	2037.9 ± 5.6	0.102 ± 0.171	445 ± 55	122 ± 7	277 ± 62	55 ± 2	This work
	60.3 ± 7.9	2031.7 ± 18.4	0.041 ± 0.46	462 ± 18	119 ± 3	227 ± 122	53 ± 2	
HIP 11253	82.18	2026.35	0.283	378	87.6	278.8	109.7	Docobo & Ling (2012)
	84.48 ± 0.86	2026.80 ± 0.2184	0.288 ± 0.0054	392.1 ± 8	86.95 ± 0.16	276.11 ± 0.27	108.61 ± 0.25	Aljboor & Taani (2023)
	45.4 ± 1.8	2025.9 ± 0.1	0.871 ± 0.012	272 ± 10	47 ± 4	296 ± 5	129 ± 3	This work
HIP 11352	11.15 ± 0.57	1998.07 ± 0.19	0.161 ± 0.022	159 ± 5	18.02 ± 0.46	163.25 ± 7.20	67.74 ± 0.15	Hönig & Tschamuter (2005)
	6.85 ± 0.05	1995.12 ± 0.06	0.284 ± 0.006	100 ± 1	15.1 ± 0.9	4.4 ± 1.6	50.0 ± 0.6	Balega et al. (2005, 2006a)
	6.93	2015.822	0.291	99	16.0	2.8	49.9	Docobo & Ling (2019)
	2533^d $\pm 5^d$	2008.93 ± 0.03	0.300 ± 0.005			163.0 ± 2.0	50.0	Griffin (2018)
	6.94 ± 0.01	1995.06 ± 0.01	0.290 ± 0.003	99.9 ± 0.6	13.65 ± 0.68	7.53 ± 0.79	51.07 ± 0.56	Al-Tawalbeh et al. (2021)
	6.941 ± 0.007	1995.05 ± 0.02	0.298 ± 0.003	99 ± 1	14.0 ± 0.7	6.2 ± 0.9	51 ± 1	This work
	19.414 ± 0.209	2007.132 ± 0.198	0.032 ± 0.009	100.4 ± 2.2	171.4 ± 0.3	126.2 ± 24.1	101.7 ± 0.3	Cvetković & Pavlović (2017)
HIP 14929	9.61 ± 0.02	2005.81 ± 0.04	0.812 ± 0.005	60.8 ± 0.8	365.4 ± 0.5	215.4 ± 0.7	115 ± 1	This work

Table 3
Fundamental Parameters of the Objects

Object	Δm_{550} , (mag)	M_A , (mag)	Sp_A	\mathfrak{M}_A , \mathfrak{M}_\odot	M_B , (mag)	Sp_B	\mathfrak{M}_B , \mathfrak{M}_\odot	$\Sigma \mathfrak{M}$, \mathfrak{M}_\odot	Parallax Source and Value (mas)	References
Chara 122Aa	6.00							125.13 ± 218.34	Hipparcos	Cvetković et al. (2008)
	1.35 ± 0.05	-1.52 ± 0.05	B2.5V	6.1	-0.17 ± 0.07	B8V	3.4	33 ± 22	Hipparcos	This work
		-1.51 ± 0.05	B2.5V	6.1	-0.16 ± 0.07	B8V	3.4	33 ± 10	Gaia DR2	
		-1.20 ± 0.05	B3V	5.4	0.15 ± 0.07	B8V	3.4	21 ± 8	Gaia DR3	
									3.0041 \pm 0.3539	
GJ 3010	0.72 ± 0.19	13.1 ± 0.2	M4.5V	0.18	13.8 ± 0.3	M4.5V	0.18	0.29 ± 0.03	Dittmann et al. (2014)	This work
		12.6 ± 1.4	M4V	0.22	13.4 ± 1.4	M4.5V	0.18	0.57 ± 0.04	Riedel et al. (2014)	
		12.7 ± 0.2	M4V	0.22	13.4 ± 0.3	M4.5V	0.18	0.53 ± 0.02	Gaia DR2	
									55.2555 \pm 0.7612	
HIP 1987	2.82	4.4	G0	1.2	7.2	K4	0.8	1.3 ± 0.2	Hipparcos	Cvetković (2011)
	2.9 ± 0.1	4.4 ± 0.1	G0V	1.08	7.3 ± 0.2	K5V	0.68	1.2 ± 0.2	Hipparcos	This work
		4.0 ± 0.1	F7V—	0.21—	6.8 ± 0.2	K4V	0.72	2.2 ± 0.2	Gaia DR2	
		4.2 ± 0.1	F8V	1.18	7.1 ± 0.2	K4.5V	0.71	1.6 ± 0.1	Gaia DR3	
		4.1 ± 0.1	F9V	1.14	7.0 ± 0.2	K4.5V	0.71	1.8 ± 0.3	Cvetković (2011)	
									19.96 \pm 1.13	
GJ 3076			M5.0	0.150		M6.0	0.120			Janson et al. (2012)
				0.10 ± 0.03			0.04 ± 0.01	0.45 ± 0.06		Janson et al. (2014a)
	1.23 ± 0.13	13.5 ± 0.1	M4.5V	0.18	14.8 ± 0.2	M5V— M5.5V	0.16— 0.12	0.15 (0.14) ± 0.12 (0.07)	Dittmann et al. (2014)	This work
		13.0 ± 0.1	M4V— M4.5V	0.22— 0.18	14.3 ± 0.2	M5V	0.16	0.31 (0.28) ± 0.21 (0.10)	Riedel et al. (2014)	
HIP 11253		9.11	G0	1.06	12.62	K4.5	0.70		Hipparcos	Al-Wardat & Wid- yan (2009)
				1.12			0.76			Tokovinin (2014a, 2014b)
		4.16 4.30	F9 F9	1.09 1.10	6.39 6.30	K3 K3	0.59 0.61	1.68 1.71	Gaia DR2 Gaia EDR3	Aljboor & Taani (2023)
	2.7 ± 0.1	4.3 ± 0.1	F9.5V— G0V	1.11— 1.08	7.1 ± 0.1	K4V— K4.5V	0.72— 0.71	2.2 ± 0.5	Hipparcos	This work
		4.6 ± 0.1	G1V— G2V	1.07— 1.02	7.4 ± 0.1	K5V	0.68	1.4 ± 0.2	Gaia DR2	
		4.5 ± 0.1	G0V— G1V	1.08— 1.07	7.3 ± 0.1	K5V	0.68	1.6 ± 0.2	Gaia DR3	
									18.9878 \pm 0.6268	
									18.1854 \pm 0.2130	
HIP 11352		5.5	G8		5.7	G9		1.71 ± 0.27	Hipparcos	Balega et al. (2006a)
			G7	0.93		G9	0.89		Hipparcos	Al-Wardat (2009)

Table 3
(Continued)

Object	Δm_{550} , (mag)	M_A , (mag)	Sp_A	\mathfrak{M}_A , \mathfrak{M}_\odot	M_B , (mag)	Sp_B	\mathfrak{M}_B , \mathfrak{M}_\odot	$\Sigma \mathfrak{M}$, \mathfrak{M}_\odot	Parallax Source and Value (mas)	References
				± 0.05			± 0.05			
		5.10	G5V	0.99	0.93	G7V	0.95		DR2	Al-Tawalbeh et al. (2021)
		± 0.13		± 0.15	± 0.05		± 0.13			
	0.38 ± 0.17	5.5 ± 0.2	G9V	0.9	5.9 ± 0.2	K1V	0.85	1.4 ± 0.2	Hipparcos 24.31 \pm 0.99	This work
		5.4 ± 0.2	G8V	0.94	5.7 ± 0.2	K0V	0.87	1.76 ± 0.06	Gaia DR2 22.5156 \pm 0.1082	
		5.4 ± 0.2	G8V	0.94	5.7 ± 0.2	K0V	0.87	1.77 ± 0.06	Gaia DR3 22.4940 \pm 0.1363	
		5.8	K0.5V	0.86	6.2	K2V	0.78	0.93	Hönig & Tscharnu- ter (2005)	
		± 0.2			± 0.2			± 0.03	27.9 \pm 0.1	
		5.3 ± 0.2	G8V	0.94	5.7 ± 0.2	K0V	0.87	1.9 ± 0.1	Piccotti et al. (2020) 22.0393 \pm 0.3926	
HIP 14929	0.53 ± 0.25	4.1 ± 0.2	F8V	1.18	4.6 ± 0.4	G1V	1.07	2.0 ± 0.6	Hipparcos 10.60 \pm 0.97	This work
		3.8 ± 0.2	F7V	1.21	4.3 ± 0.3	F9.5V	1.11	2.9 ± 0.1	Gaia DR2 9.4238 \pm 0.0685	
		3.8 ± 0.2	F7V	1.21	4.4 ± 0.3	F9.5V— G0V	1.11— 1.08	2.8 ± 0.1	Gaia DR3 9.5577 \pm 0.0581	

$\Delta\theta = 2^\circ.2$. The data (29 measurements) cover almost all phases of the orbital period ($\approx 70\%$) and a little more than one revolution passed from the first to the last observation. Therefore we classify the orbit as “good” (Grade 2). The masses obtained by two independent methods do not agree with each other for all three parallaxes. In this case, we can assume either that the parallaxes are incorrect or that the components are not main sequence stars. In any case, further monitoring of the system is required.

GJ 3010 (00^h08^m53^s 9 + 20°50′25″ 5; BEU 1, G 131-26) was resolved as a binary for the first time by Beuzit et al. (2004). Further monitoring of the object made it possible to calculate the orbital parameters and masses of the system and its components (Janson et al. 2014a, Vrijmoet et al. 2022, Calissendorff et al. 2022). The orbital solution was slightly improved after analyzing 13 new measurements (Figure 1, top-middle panel, compared to an orbit constructed using a grid method by Calissendorff et al. 2022). In this case, there is no doubt about the classification of the orbit as “definitive” (Grade 1). Only Dittmann et al. (2014), Riedel et al. (2014) ($\pi_{\text{Ditt}} = 67.5 \pm 2.7$ mas and $\pi_{\text{Ried}} = 54.13 \pm 1.35$ mas) and Gaia DR2 (which is close to the Riedel et al. (2014) parallax) parallaxes are available for the calculation of fundamental parameters. Also we used the magnitude difference of the components in 800 bandpass, assuming that its value is close to the one in 550 bandpass. The obtained masses are in good

agreement with each other for Gaia DR2 parallax and with those previously published (Janson et al. 2014a; Vrijmoet et al. 2022; Calissendorff et al. 2022), taking into account limits and our assumptions.

HIP 1987 (00^h25^m08^s 7 + 48°02′50″ 6; HD 2057, HDS 56) is a triple system with outer period $\log P_L = 4.02$ (Tokovinin 2008). The first orbital solution for a wide pair of components was calculated by Cvetković (2011) based on 11 measurements. It was unresolved in 1997.7206 by Mason et al. (1999). This date is close to the periastron passage. After adding new data (30 measurements), it became clear that measurements by Balega et al. (2007, 2013) had a quadrant ambiguity. The 46 measurements almost completely cover all orbital phases ($\approx 75\%$), which makes it possible to obtain a “definitive” (Grade 1) orbital solution (Figure 1, top-right panel). The residuals for ρ and θ are 5.3 mas and $1^\circ.2$, respectively. One revolution has passed. The fundamental parameters calculated using the four parallax values are in better agreement when the Gaia DR2 parallax and dynamic parallax by Cvetković (2011) are applied. Since the orbital solution was improved slightly, the masses obtained in this study are similar to those published by Malkov et al. (2012), Tokovinin (2014a, 2014b).

GJ 3076 (01^h11^m25^s 4 + 15°26′21″ 5; BEU 2, LP 467-16) was resolved for the first time by Beuzit et al. (2004) and its first period was estimated by Janson et al. (2014a)

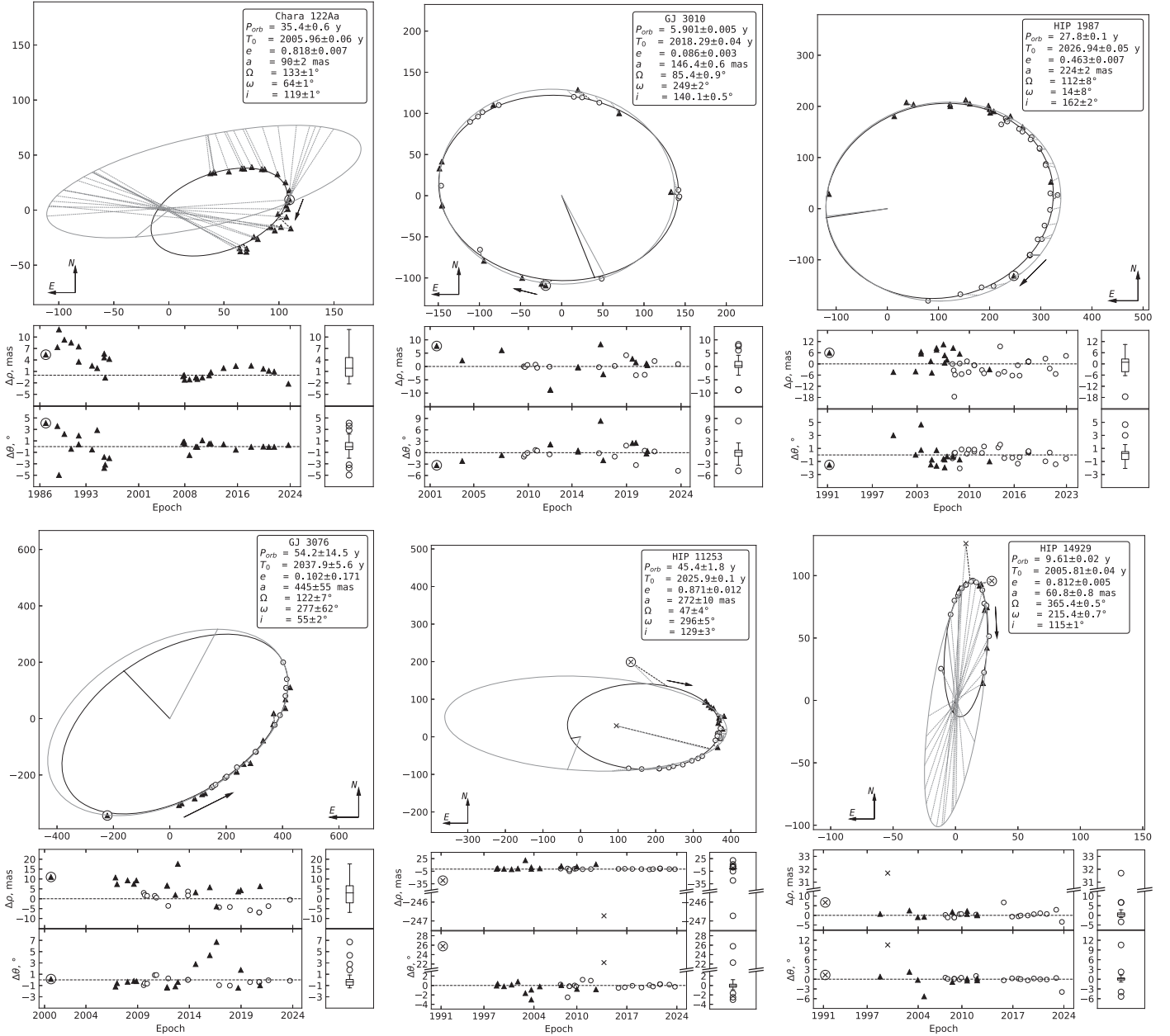


Figure 1. Orbital solutions. The orbits constructed in this work are marked in black. The previously published orbits are shown in gray. Triangles correspond to the published data; open circles—data obtained in this study; crosses—data with large residuals; a point placed in a large circle is the first measurement for the system. The arrow shows the direction of motion of the secondary. $\Delta\rho$ and $\Delta\theta$ are residuals of angular separation and position angle respectively showing the difference between the observed and model value. The dashed line on the residuals plots indicates the orbital solution. Boxplots display the distribution of data based on a five-number summary (“minimum”, first quartile (Q1), median, third quartile (Q3), and “maximum”) and outliers.

($P_{\text{orb}} = 30\text{--}40$ yr). The first complete set of orbital parameters for this system was obtained by Calissendorff et al. (2022). Adding 15 new measurements still does not allow for the construction of an unambiguous orbit of the object. The orbital solution depends on the weights we choose for each measurement. We selected two that fit the observational data

well (Table 2) and have the smallest residuals in terms of separation and position angle. The orbit of GJ 3076 can only be classified as “reliable” (Grade 3). Even the 31 measurements available to us do not allow for obtaining the precise orbital parameters with confidence. To calculate the fundamental parameters, we used the magnitude difference in 800 bandpass,

which is close to the estimation of the magnitude difference in 500 bandpass obtained by Beuzit et al. (2004). Only parallaxes by Dittmann et al. (2014) (58.0 ± 7.30 mas) and Riedel et al. (2014) (45.79 ± 1.78 mas) are available for this object. Figure 1 (bottom-left panel) shows a comparison of the two orbits constructed in this work (the orbit with period of 54.2 yr is marked in black, and that with a period of 60.3 yr—in gray). The value of the mass sum for an orbital solution with a period of 60.3 yr is shown in brackets in Table 3. Since the orbit is not precise enough yet to draw definitive conclusions, we cannot make specific conclusions about masses and parallaxes, but the parallax by Riedel et al. (2014) results in more consistent parameters. Further monitoring of this system is definitely required.

HIP 11253 ($02^{\text{h}}24^{\text{m}}51^{\text{s}}.1 + 30^{\circ}38'48''.3$; HD 14874, HDS 314) is a binary with components of the G0 and K4 spectral types (Balega et al. 2002). Later Al-Wardat & Widyana (2009) revealed that the secondary is not a main sequence star. The first orbital solution for the system was obtained by Docobo & Ling (2012), and then the orbital period equal to 75.012 yr was suggested (Tokovinin 2014a, 2014b). We did not use measurement 2013.7971 by Kehrli et al. (2017) in the study; even changing the positional angle by 180° does not help (Figure 1, bottom-middle panel). New data (19 measurements) allow for the obtaining of orbital parameters that are radically different from the previous ones. Slightly more than 70% of orbital phases are covered by 32 measurements. The residuals for ρ and θ are 5.1 mas and $0^{\circ}.9$, respectively. Even though the system has not yet completed a full revolution, we can classify this orbital solution as “definitive” (Grade 1). The calculated masses agree best with each other if Gaia DR3 parallax is applied, although they are in agreement for other parallaxes as well.

HIP 14929 ($03^{\text{h}}12^{\text{m}}32^{\text{s}}.9 + 18^{\circ}56'36''.8$; HD 19895, HDS 408) is a binary consisting of F8-F9 stars (Balega et al. 2002), the orbit of which was constructed for the first time by Cvetković & Pavlović (2017). Analysis of new speckle interferometric data (17 measurements) showed that the position angles of the measurements by ESA (1997), Mason et al. (2001), Balega et al. (2002, 2007, 2013) should be changed by 180° . Indeed, it is easy to make a mistake in determining the position of the secondary due to the small separation between the components and the low magnitude difference between them. As a result the orbital period calculated for this system differs significantly from its previous estimate (Figure 1, bottom-right panel). The residuals regarding the orbital solution are $\Delta\rho = 1.8$ mas and $\Delta\theta = 1^{\circ}.4$. There are 27 measurements covering more than three orbital revolutions and approximately 85% of orbital phases. The orbit is classified as “definitive” (Grade 1) based on these factors. Although the parallaxes have almost the same values, the obtained parameters are in better agreement with each other when using the Hipparcos parallax.

3.1. Combined Solutions

HIP 11352 ($02^{\text{h}}26^{\text{m}}09^{\text{s}}.6 + 34^{\circ}28'10''.0$; HD 15013, HDS 318) is a binary consisting of components of G8 and G9 spectral types ($M_A = 5.5$ mag and $M_B = 5.7$ mag, Balega et al. 2002). The first two estimates of orbital solutions with periods of 6 and 11 years were obtained by Hönl & Tscharnuter (2005). Due to the short period of the system and the constantly increasing amount of astrometric and spectroscopic data, the orbital and fundamental parameters previously published by Balega et al. (2005), Al-Wardat (2009), Tokovinin (2014a, 2014b), Malkov et al. (2012), Griffin (2018), Piccotti et al. (2020), Al-Tawalbeh et al. (2021) have similar values. Our orbit, slightly improved after adding new data (17 measurements), and masses are not an exception.

The combined orbit for *HIP 11352* (Figure 2) is constructed, since both astrometric measurements and radial velocities are available and the data cover almost all phases of the orbital period. Quadrant ambiguities were detected in measurements 1999.8856 and 2000.7622 by Horch et al. (2002) and 2001.7643 by Horch et al. (2008), which were also reported by Hönl & Tscharnuter (2005) and Balega et al. (2005). We used radial velocities from the SB9: 9th Catalog of spectroscopic binary orbits (Pourbaix et al. 2004) and references therein). Since the orbital solution is combined, $K_1 = -7.61 \pm 0.04 \text{ km s}^{-1}$, $K_2 = -7.86 \pm 0.04 \text{ km s}^{-1}$ and $\gamma = -0.67 \pm 0.02 \text{ km s}^{-1}$ are added to the parameters from Table 3. The orbit of *HIP 11352* is “definitive” (Grade 1). In addition to the Hipparcos, and Gaia DR2 and DR3 parallaxes, we used the values calculated by Hönl & Tscharnuter (2005) and Piccotti et al. (2020). Based on the obtained mass sums and masses of components, we can conclude that they match better when using parallax by Piccotti et al. (2020).

4. Discussion

The number of measurements of positional parameters for the objects under study has increased significantly due to the monitoring of speckle interferometric binaries carried out by our group at the 6 m telescope since 2007. New measurements are equal to or greater in number than those previously published for almost all systems: 16 new versus 13 published one for Chara 122Aa, 13 versus 13 for GJ 3010, 30 versus 16 for *HIP 1987*, 15 versus 16 for GJ 3076, 19 versus 14 for *HIP 11253*, 17 versus 25 for *HIP 11352*, and 17 versus 11 for *HIP 14929*. This made it possible to construct completely new orbits for Chara 122Aa, *HIP 11253*, and *HIP 14929*. Also, the contribution of accurate reconstruction of the position of the secondary when obtaining new orbital parameters should not be diminished. But at the same time, it is worth noting that even a large amount of observational data does not allow for constructing an accurate orbit in exceptional cases (GJ 3076). The classification of orbital solutions shows a high percentage of “definitive” (Grade 1) orbits. However, there are still objects

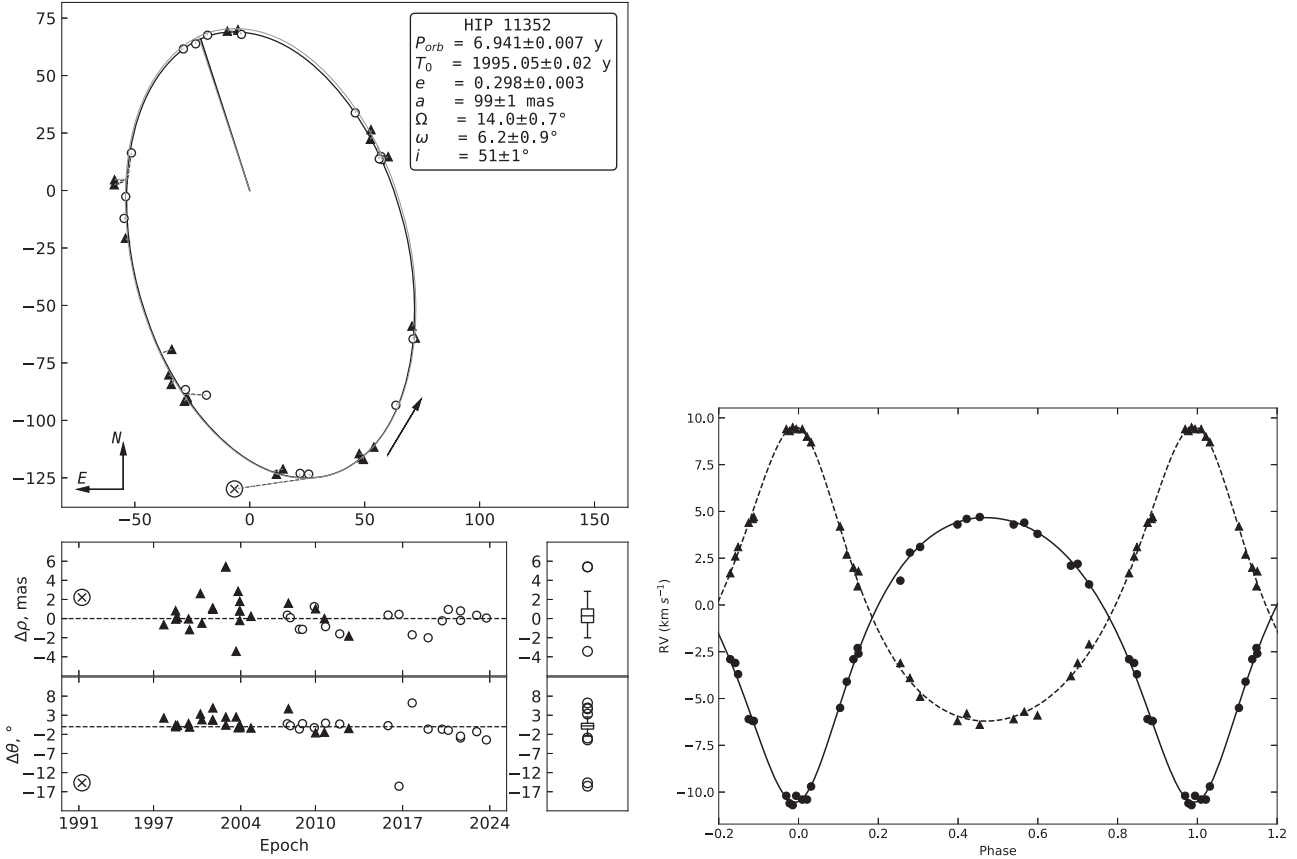


Figure 2. Combined orbital solutions for HIP 11352. Designations on the left panel are described in the caption of Figure 1. Circles on the right panel refer to the radial velocities of the primary and triangles to the secondary.

(Chara 122Aa and GJ 3076) for which the study indicates the need to continue their monitoring.

The fundamental parameters of only HIP 11253 are in best agreement when Gaia DR3 parallax is applied, and for GJ 3010 and GJ 3076 this parallax is absent. In the case of Chara 122Aa, the masses are not consistent at all for any parallax. We hope that the appearance of modern parallaxes (by the Gaia mission?) will also help to understand the existing problems.

Acknowledgments

We obtained part of the observed data on the unique scientific facility Big Telescope Alt-azimuthal of SAO RAS as well as conducted data processing with the financial support of grant No. 075-15-2022-262 (13.MNPMU.21.0003) of the Ministry of Science and Higher Education of the Russian Federation.

ORCID iDs

Arina Mitrofanova <https://orcid.org/0000-0002-2305-5499>

References

- ESA 1997, in ESA Special Publication, The HIPPARCOS and TYCHO catalogues. Astrometric and photometric star catalogues derived from the ESA HIPPARCOS Space Astrometry Mission (Paris: European Space Agency)
- Al-Tawalbeh, Y. M., Hussein, A. M., Taani, A. A., et al. 2021, *AstBu*, **76**, 71
- Al-Wardat, M. A. 2009, *AN*, **330**, 385
- Al-Wardat, M. A., & Widyana, H. 2009, *AstBu*, **64**, 365
- Aljboor, H., & Taani, A. 2023, *RAA*, **23**, 075018
- Balega, I., Balega, Y. Y., Maksimov, A. F., et al. 2004, *A&A*, **422**, 627
- Balega, I., Bonneau, D., & Foy, R. 1984, *A&AS*, **57**, 31
- Balega, I. I., & Balega, Y. Y. 1985, *PAZh*, **11**, 112
- Balega, I. I., Balega, Y. Y., Gasanova, L. T., et al. 2013, *AstBu*, **68**, 53
- Balega, I. I., Balega, Y. Y., Hofmann, K. H., et al. 2002, *A&A*, **385**, 87
- Balega, I. I., Balega, Y. Y., Hofmann, K. H., et al. 2006a, *A&A*, **448**, 703
- Balega, I. I., Balega, Y. Y., Hofmann, K. H., et al. 2005, *A&A*, **433**, 591
- Balega, I. I., Balega, Y. Y., Maksimov, A. F., et al. 2006b, *BSAO*, **59**, 20
- Balega, I. I., Balega, Y. Y., Maksimov, A. F., et al. 2007, *AstBu*, **62**, 339
- Balega, I. I., Balega, Y. Y., Maksimov, A. F., et al. 1999, *A&AS*, **140**, 287
- Beddoes, D. R., Dainty, J. C., Morgan, B. L., & Scaddan, R. J. 1976, *JOSA*, **66**, 1247
- Beuzit, J. L., Ségransan, D., Forveille, T., et al. 2004, *A&A*, **425**, 997
- Bonneau, D., Blazit, A., Foy, R., & Labeyrie, A. 1980, *A&AS*, **42**, 185
- Busso, G., Cacciari, C., Carrasco, J. M., et al. 2018, Gaia DR2 Documentation Chapter 5: Photometry, *Tech. Rep. 5*, European Space Agency, Paris
- Calissendorff, P., Janson, M., & Bonnefoy, M. 2020, *A&A*, **642**, A57
- Calissendorff, P., Janson, M., Rodet, L., et al. 2022, *A&A*, **666**, A16

- Cortés-Contreras, M., Béjar, V. J. S., Caballero, J. A., et al. 2017, *A&A*, 597, A47
- Cvetković, Z. 2011, *AJ*, 141, 116
- Cvetković, Z., Novaković, B., & Todorović, N. 2008, *NewA*, 13, 125
- Cvetković, Z., & Pavlović, R. 2017, *AJ*, 154, 273
- Davidson, J. W., Horch, E. P., Majewski, S. R., et al. 2024, *AJ*, 167, 117
- Dittmann, J. A., Irwin, J. M., Charbonneau, D., & Berta-Thompson, Z. K. 2014, *ApJ*, 784, 156
- Docobo, J. A., & Ling, J. F. 2012, *Inf. Circ.*, 177, 1
- Docobo, J. A., & Ling, J. F. 2019, *Inf. Circ.*, 196, 1
- Fu, H.-H., Hartkopf, W. I., Mason, B. D., et al. 1997, *AJ*, 114, 1623
- Gaia Collaboration, Brown, A. G. A., Vallenari, A., et al. 2018, *A&A*, 616, A1
- Gaia Collaboration, Vallenari, A., Brown, A. G. A., et al. 2023, *A&A*, 674, A1
- Griffin, R. F. 2018, *Obs*, 138, 192
- Hartkopf, W. I., Mason, B. D., & Worley, C. E. 2001, *AJ*, 122, 3472
- Hartkopf, W. I., McAlister, H. A., & Franz, O. G. 1992, *AJ*, 104, 810
- Hartkopf, W. I., McAlister, H. A., Mason, B. D., et al. 1997, *AJ*, 114, 1639
- Hartkopf, W. I., Mason, B. D., McAlister, H. A., et al. 2000, *AJ*, 119, 3084
- Hönig, S. F., & Tschamner, W. M. 2005, *AJ*, 129, 1663
- Horch, E., Ninkov, Z., van Altena, W. F., et al. 1999, *AJ*, 117, 548
- Horch, E. P., Bahi, L. A. P., Gaulin, J. R., et al. 2012, *AJ*, 143, 10
- Horch, E. P., Falta, D., Anderson, L. M., et al. 2010, *AJ*, 139, 205
- Horch, E. P., Gomez, S. C., Sherry, W. H., et al. 2011, *AJ*, 141, 45
- Horch, E. P., Meyer, R. D., & van Altena, W. F. 2004, *AJ*, 127, 1727
- Horch, E. P., Robinson, S. E., Meyer, R. D., et al. 2002, *AJ*, 123, 3442
- Horch, E. P., van Altena, W. F., Cyr, W. M. J., et al. 2008, *AJ*, 136, 312
- Horch, E. P., Veillette, D. R., Baena Gallé, R., et al. 2009, *AJ*, 137, 5057
- Horch, E. P., van Altena, W. F., Demarque, P., et al. 2015, *AJ*, 149, 151
- Horch, E. P., Casetti-Dinescu, D. I., Camarata, M. A., et al. 2017, *AJ*, 153, 212
- Horch, E. P., Broderick, K. G., Casetti-Dinescu, D. I., et al. 2021, *AJ*, 161, 295
- Hussein, A. M., Abu-Alrob, E. M., Mardini, M. K., Alslaihat, M. J., & Al-Wardat, M. A. 2024, *AdSpR*, 73, 1103
- Janson, M., Bergfors, C., Brandner, W., et al. 2014a, *ApJ*, 789, 102
- Janson, M., Bergfors, C., Brandner, W., et al. 2014b, *ApJS*, 214, 17
- Janson, M., Hormuth, F., Bergfors, C., et al. 2012, *ApJ*, 754, 44
- Kehrli, M., David, H., Drake, E., et al. 2017, *JDSO*, 13, 122
- Labeyrie, A. 1970, *A&A*, 6, 85
- Lohmann, A. W., Weigelt, G., & Wirtzner, B. 1983, *ApOpt*, 22, 4028
- Maksimov, A. F., Balega, Y. Y., Dyachenko, V. V., et al. 2009, *AstBu*, 64, 296
- Malkov, O. Y., Tamazian, V. S., Docobo, J. A., & Chulkov, D. A. 2012, *A&A*, 546, A69
- Masda, S., Yousef, Z. T., Al-Wardat, M., & Al-Khasawneh, A. 2023, *RAA*, 23, 115005
- Mason, B. D., Hartkopf, W. I., Holdenried, E. R., & Rafferty, T. J. 2001, *AJ*, 121, 3224
- Mason, B. D., Martin, C., Hartkopf, W. I., et al. 1999, *AJ*, 117, 1890
- Mason, B. D., Tokovinin, A., Mendez, R. A., & Costa, E. 2023, *AJ*, 166, 139
- McAlister, H. A. 1977, *ApJ*, 215, 159
- McAlister, H. A., Hartkopf, W. I., Sowell, J. R., Dombrowski, E. G., & Franz, O. G. 1989, *AJ*, 97, 510
- McAlister, H. A., Mason, B. D., Hartkopf, W. I., & Shara, M. M. 1993, *AJ*, 106, 1639
- McAlister, H., Hartkopf, W. I., & Franz, O. G. 1990, *AJ*, 99, 965
- Mitrofanova, A., Dyachenko, V., Beskakotov, A., et al. 2021, *AJ*, 162, 156
- Mitrofanova, A., Dyachenko, V., Beskakotov, A., et al. 2020a, *RAA*, 20, 187
- Mitrofanova, A., Dyachenko, V., Beskakotov, A., et al. 2020b, *AJ*, 159, 266
- Monet, D. G. 1977, *ApJ*, 214, L133
- Morgan, B. L., Beddoes, D. R., Scaddan, R. J., & Dainty, J. C. 1978, *MNRAS*, 183, 701
- Novakovic, B. 2006, *IAUDS*, 160, 1
- Perryman, M. A. C., Lindegren, L., Kovalevsky, J., et al. 1997, *A&A*, 323, L49
- Piccotti, L., Docobo, J. Á., Carini, R., et al. 2020, *MNRAS*, 492, 2709
- Pluzhnik, E. A. 2005, *A&A*, 431, 587
- Pourbaix, D., Tokovinin, A. A., Batten, A. H., et al. 2004, *A&A*, 424, 727
- Riddle, R. L., Tokovinin, A., Mason, B. D., et al. 2015, *ApJ*, 799, 4
- Riedel, A. R., Finch, C. T., Henry, T. J., et al. 2014, *AJ*, 147, 85
- Tango, W. J., Davis, J., Thompson, R. J., & Hanbury, R. 1979, *PASA*, 3, 323
- Tokovinin, A. 1992, in *ASP Conf. Ser. 32, IAU Colloq. 135: Complementary Approaches to Double and Multiple Star Research*, ed. H. A. McAlister & W. I. Hartkopf (San Francisco, CA: ASP), 573
- Tokovinin, A. 2008, *MNRAS*, 389, 925
- Tokovinin, A. 2014a, *AJ*, 147, 86
- Tokovinin, A. 2014b, *AJ*, 147, 87
- Tokovinin, A. 2017, *ApJ*, 844, 103
- Tokovinin, A. A. 1978, *PAZh*, 4, 381
- Tokovinin, A., Mason, B. D., Mendez, R. A., & Costa, E. 2022, *AJ*, 164, 58
- Tokovinin, A., Mason, B. D., Mendez, R. A., et al. 2021, *AJ*, 162, 41
- van Leeuwen, F. 2007, *A&A*, 474, 653
- Vrijmoet, E. H., Tokovinin, A., Henry, T. J., et al. 2022, *AJ*, 163, 178
- Weigelt, G. P. 1978, *A&A*, 68, L5